INTERNATIONAL JOURNAL FOR NUMERICAL METHODS IN FLUIDS, VOL. 9, 1087–1098 (1989)

THREE-DIMENSIONAL REDUCED NAVIER–STOKES SOLUTIONS FOR SUBSONIC SEPARATED AND NON-SEPARATED FLOWS, USING A GLOBAL PRESSURE RELAXATION PROCEDURE

R. COHEN* AND P. K. KHOSLA
University of Cincinnati, Cincinnati, OH 45221, U.S.A.

SUMMARY

The reduced Navier–Stokes and thin layer approximations to the Navier–Stokes equations are used to obtain solutions for viscous subsonic three-dimensional flows. A spatial marching method is combined with a direct sparse matrix solver to obtain successive solutions in a global relaxation process. Results have been obtained for flow fields with and without regions of flow reversal.

KEY WORDS RNS Separation Direct solver

1. INTRODUCTION

Calculation of viscous subsonic flow-fields about three-dimensional geometries are generally carried out by solution of the full Navier–Stokes (NS) equations. In general, three-dimensional solvers encounter many difficulties associated with the choice of difference scheme, the method of solution, the degree of coupling of the dependent variables and the manner in which the boundary conditions are satisfied.[1] Recent research efforts have focused on the reduced (RNS) or thin layer (TL) approximations to the full equations to obtain solutions for three-dimensional configurations. It is well established from work with two-dimensional flows that in many cases, for large-Reynolds-number flows, the RNS and TL equations produce results comparable with the full equations, but offer several major advantages,[1–5] e.g. reduced computer storage, a simple boundary-layer-like solution procedure, only an outflow boundary condition on pressure, and location of the computational boundaries closer to the region of strong pressure interaction.

The RNS equations are derived by order-of-magnitude or perturbation analysis of the NS equations and are applicable to high-Reynolds-number flows with a dominant flow direction. It must be emphasized that the RNS model, although introduced as an asymptotic approximation, can be utilized to solve the full NS equations where the discarded terms are retained via a deferred corrector approach. These equations represent a composite of the Euler and boundary layer assumptions in a single system of equations. Inclusion of the normal (y) inviscid momentum equation and the streamwise pressure gradient P_x provide a consistent mechanism for

* Permanent address: University of Sydney, NSW 2006, Australia.

0271–2091/89/091087–12$06.00

Received 7 April 1988
Revised 20 September 1988

viscous–inviscid interaction. In corner regions or for internal flows, cross-flow diffusion in the normal momentum equation can also become important and must be included.

In view of the structure of the equations, the RNS system has been confused with the more commonly known parabolized Navier–Stokes (PNS) system. It must be pointed out that for subsonic flows, the RNS system is elliptic. The ellipticity arises through the interacting axial pressure gradient. Solution of the RNS system as an initial value problem, using marching techniques, yields departure solutions. Lubard and Helliwell[6] show that the process requires the streamwise marching step size Δx to be larger than some minimum size, which Rubin and Lin[2] have shown is proportional to the thickness of the subsonic layer. This would be the entire normal extent of the flow field for fully subsonic flows. This step size limitation is removed if the unknown pressure gradient term is discarded. In order to obtain solutions where this term is retained, the elliptic character of the governing equations must be reflected in the discretization. As shown by Rubin[1] or Rubin and Lin,[2] the axial pressure gradient should be forward or flux differenced so that a downstream boundary condition on pressure needs to be prescribed. With this formulation, a marching procedure is embedded within a global pressure relaxation technique. This allows propagation of upstream influence in the flow field to be taken into account. In regions of attached flow, only the pressure need be stored globally. Regions of separated flow require storage of the streamwise and cross-flow velocity components as well. This can be extremely important for three-dimensional flows, where storage requirements must be minimized.

The relaxation process involves calculation of solutions on successive cross-planes and updating of the global pressure field. Global iteration is governed entirely by the pressure solution. The flow velocities are regenerated for each global solution pass. In two dimensions this technique has been applied to many flows, including complex configurations with large longitudinal curvature, mixing shear layers, large regions of separated flow, base flows and jet interaction. In three dimensions Raven and Hoekstra[7] have solved the RNS equations for the flow about a ship stern. Rosenfeld *et al.*[8] have also developed a similar procedure using reduced equations to calculate the flow field about prolate spheroids at angle of attack. Additional cross-flow numerical viscosity is added to the equations in Reference 8.

In the present paper the RNS equations have been formulated to solve the flow about various three-dimensional configurations. Section 2 describes the governing equations, the discretization schemes and the solution method. In Secion 3 solutions are shown for a finite edge flat plate, the flow along an axial corner and the flow over a trigonometric bump.

2. GOVERNING EQUATIONS AND SOLUTION PROCEDURE

The incompressible forms of the RNS equations are appropriately non-dimensionalized and written in primitive variables for the continuity and three momentum equations. The dominant flow is assumed to be in the x direction. The cross-plane is defined by y and z.

Continuity

$$u_x + v_y + w_z = 0,$$

x (streamwise) momentum

$$P_x + uu_x + vu_y + wu_z = \frac{1}{Re}[u_{yy} + u_{zz}],$$

y-momentum

$$P_y + uv_x + vv_y + wv_z = \frac{1}{Re}[v_{yy} + v_{zz}],$$

z-momentum

$$P_z + uw_x + vw_y + ww_z = \frac{1}{Re}[w_{yy} + w_{zz}],$$

where u is the streamwise velocity component, v and w are the secondary velocity components, P is the pressure and Re is the Reynolds number. The left-hand side of the above system represents the Euler equations. If the right-hand side of the y-momentum equation is omitted, then the resulting system is the RNS equations applicable to flows over a surface with a predominant normal direction. These terms need to be retained for corner-type geometries where there is no single normal direction. The boundary region (BR) equations can be obtained by prescribing the pressure and omitting the convective and viscous terms in the y-momentum equation. The boundary region equations represent a generalization of the three-dimensional boundary layer equations for flows over geometries with large transverse curvature where cross-flow diffusion plays an important role. These equations can predict secondary flow separation, but they cannot account for axial separation.

2.1. Discretization and boundary conditions

Two discretizations of the governing equations are used. The choice depends on the flow geometry.

Corner geometries. For axial corner-type geometries we retain Cartesian co-ordinates rather than use a mapping to a flat geometry. This choice was based on the fact that a clustered Cartesian grid produces maximum resolution in the corner, which is the region of interest. An orthogonal mapping, regardless of clustering, will tend to lose resolution in the corner. In Cartesian co-ordinates there is no predominant normal direction. Both the y- and z-momentum equations must retain viscous terms. The continuity equation is differenced at $(i, j-\frac{1}{2}, k-\frac{1}{2})$. The y-momentum equation is differenced at $(i, j+\frac{1}{2}, k)$ and the z-momentum equation at $(i, j, k+\frac{1}{2})$. The streamwise momentum equation is differenced at (i, j, k). Pressure can be solved for on both walls; continuity provides v on the far field y-boundary and w on the far field z-boundary. At the far field corner point, u and P are prescribed, while continuity and a zero-vorticity condition $\partial w/\partial y - \partial v/\partial z = 0$ are used to find v and w. The streamwise pressure gradient is set to zero at the downstream boundary. The boundary conditions for corner geometries are illustrated in Figure 1.

Other geometries. For geometries where the wall layer is predominantly normal to one co-ordinate direction, no viscous terms need be included in the normal (y) momentum equation. The continuity equation is differenced at grid location $(i, j-\frac{1}{2}, k)$. The streamwise (x) and cross-flow (z) momentum equations are differenced at location (i, j, k). All y- and z-derivatives in these equations are central differenced, while the term P_x is forward differenced. A general interpretation of this can be found in Reference 3. All other x-derivatives are backward differenced. The normal (y) momentum equation is differenced at $(i, j+\frac{1}{2}, k)$. The half-point differencing allows the continuity equation to be solved on the outer normal boundary to obtain v. The y-momentum equation can be solved at the body surface to obtain the pressure. At the downstream boundary the streamwise pressure gradient is set to zero. Figure 2 shows the boundary conditions for these configurations.

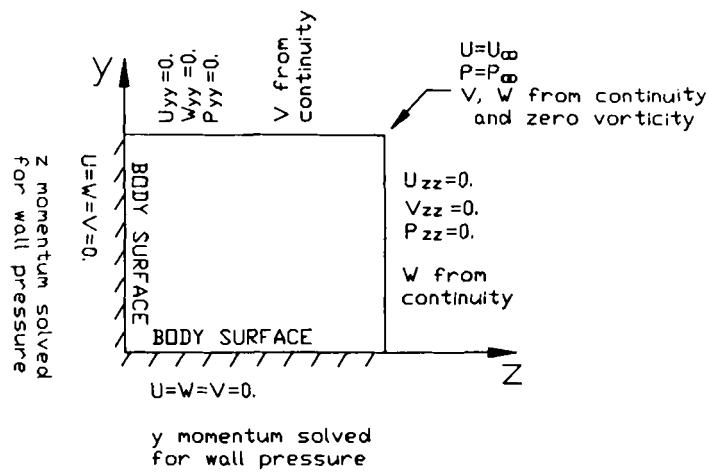

Figure 1. Boundary conditions for corner geometries

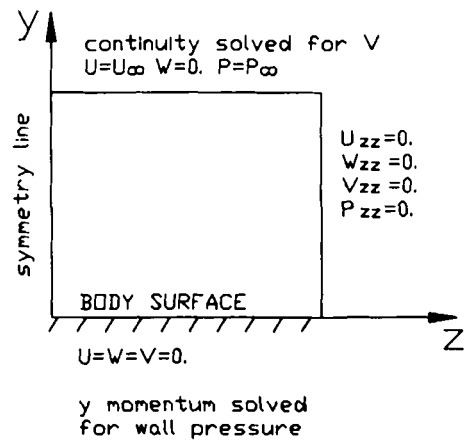

Figure 2. Boundary conditions for other geometries

2.2. *Reversed flows*

When the streamwise velocity u becomes negative, the above differencing schemes become unstable. For two-dimensional flows, forward differencing of the convective term $u(u)_x$ in the streamwise momentum equation will stabilize the system. For three-dimensional systems, the convective term $u(w)_x$ in the cross-flow momentum equation must also be forward or flux differenced. Even with flux differencing, the solution has been sensitive to initial conditions. To decrease this sensitivity, temporal terms are added to the streamwise and cross-flow momentum equations. These are rewritten as;

x (streamwise) momentum

$$u_t + P_x + u(u)_x + v(u)_y + w(u)_z = v[u_{yy} + u_{zz}],$$

z-momentum

$$w_t + P_z + u(w)_x + v(w)_y + w(w)_z = \nu[w_{yy} + w_{zz}].$$

Continuity and normal momentum equations remain unchanged. A $\Delta t = 1000$ is usually used when the initial pressure is prescribed from the inviscid solution. When the solution was partially converged, the time terms could be switched off and the relaxation process continued until a fully converged solution was attained.

2.3. *Method of solution*

The discretized equations are quasi-linearized. This results in a nine-point implicit scheme, on a grid where subscripts i, j, k refer to the x-, y- and z-direction respectively. The algebraic system is represented as

$$\mathbf{a}\boldsymbol{\phi}^n_{ij-1k} + \mathbf{b}\boldsymbol{\phi}^n_{ijk} + \mathbf{c}\boldsymbol{\phi}^n_{ij+1k} + \mathbf{d}\boldsymbol{\phi}^n_{ijk-1} + \mathbf{e}\boldsymbol{\phi}^n_{ijk+1} + \mathbf{qq}\boldsymbol{\phi}^n_{ij-1k-1} + \mathbf{rr}\boldsymbol{\phi}^n_{ij+1k-1} + \mathbf{ss}\boldsymbol{\phi}^n_{ij-1k+1} + \mathbf{tt}\boldsymbol{\phi}^n_{ij+1k+1} = \mathbf{r}_{ijk},$$

where

$$\boldsymbol{\phi}^n_{ijk} = \begin{bmatrix} u^n_{ijk} \\ w^n_{ijk} \\ v^n_{ijk} \\ p^n_{ijk} \end{bmatrix}$$

are the unknowns being solved for at global iteration number n. The coefficients **a**, **b**, **c**, **d**, **e**, **qq**, **rr**, **ss** and **tt** are 4×4 matrices. The right-hand side **r** is a vector of four elements, which consists of all known terms. Over an entire cross-plane this scheme produces a linear system, written in matrix form as

$$\mathbf{A}\boldsymbol{\Phi}^n_i = \mathbf{R},$$

where $\boldsymbol{\Phi}$ is a vector of all the unknowns $\boldsymbol{\phi}$ on the cross-plane at streamwise location x_i, **A** is a matrix of all the coefficients and **R** is a vector of all right-hand side terms **r**. This system is solved directly using a modified version of the Yale sparse matrix solver. Without any local iteration, the resulting solution is accurate to the order of the discretization.

Use of a direct solver was motivated by the need to solve a coupled set of equations. The solution technique should be as implicit as possible and also be robust. Previous experience with other implicit methods, such as the coupled strongly implicit (CSIP) method[9] and modifications thereof,[10] were found to be prone to instability. These methods tended to diverge on local iteration unless severe marching step size restrictions were enforced. Raven and Hoekstra[7] use a CSIP method in their calculations. They mention encountering convergence problems with the algorithm and so recommend enhancing the implicitness of the CSIP process. This is a step towards a 'more direct' type of solver. With the use of a direct solver, an entire cross-plane is solved non-iteratively in a single step.

The solver used in the present work is the Yale sparse matrix package (YSMP).[11] It has been successfully used by Bender and Khosla[12] and Vanka and Leaf[13] for solution of a wide range of two-dimensional problems. The package itself is an efficient set of programs for performing an LU decomposition of the coefficient matrix **A**. Only non-zero coefficients of the decomposition are stored. The non-zero elements in **A** are stored as a vector in row-wise order. An integer vector **JA** stores the column location of each element of **A**. Another integer vector **IA** contains the

starting position of each row in A. The solver requires at minimum that the main diagonal element of each row of A be non-zero. Reordering of the equations to minimize the amount of fill that is generated by the LU decomposition and tracking of the non-zeros are implicit in the package. This solver has been highly optimized for sparse matrices. Its storage requirement is less than that of any band or block solver. It does not require that the inverted matrix have any specific or regular structure. A more detailed description of the solver can be found in References 11 and 12.

Once a solution vector Φ^n is obtained, local iteration on the non-linearity can be performed before marching to the next cross-plane. This was found to be unnecessary, as the accuracy of the differencing and linearization is adequate for the global relaxation process. It was found that local iteration had a negligible effect on the global converged solution. When solution of a single cross-plane is obtained, the whole procedure is repeated for the next cross-plane. With completion of a single global pass, marching from upstream is restarted using the updated pressure field. This is continued until global convergence of the pressure field is achieved.

3. RESULTS

Comparison of the present results with experimental and other numerical solutions is limited. Current work has involved the development of a robust method that will be applicable to a wide range of prolems. Computer codes developed so far include viscous terms in all three momentum equations. Limited compressibility can be accounted for by varying the density according to an energy equation based on constant enthalpy. In some cases, refinement of finite difference grids would be required to capture all detail in the flow field. Convergence of the global relaxation process compares favourably with Rosenfeld *et al.*[8] Convergence histories for reversed and attached flows are depicted in Figures 3 and 4. To monitor convergence, the maximum change in the global pressure field has been used.

3.1. Attached flows

Results for the flow along a streamwise corner and along a flat plate of finite span have been obtained. Typical streamwise velocity profiles can be seen in Figures 5 and 6. Comparison of the present corner flow results with the asymptotic corner layer solution by Rubin and Grossman[14] show a similar profile in the far field. In Figure 7 streamwise velocity profiles are plotted against

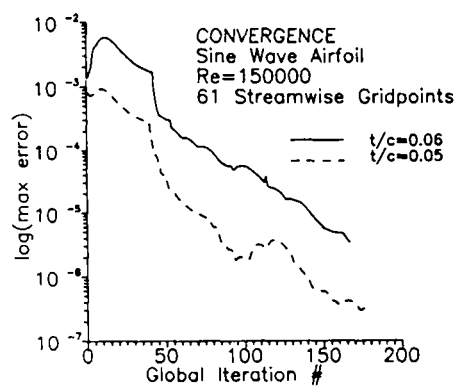

Figure 3. Convergence history: non-separated case

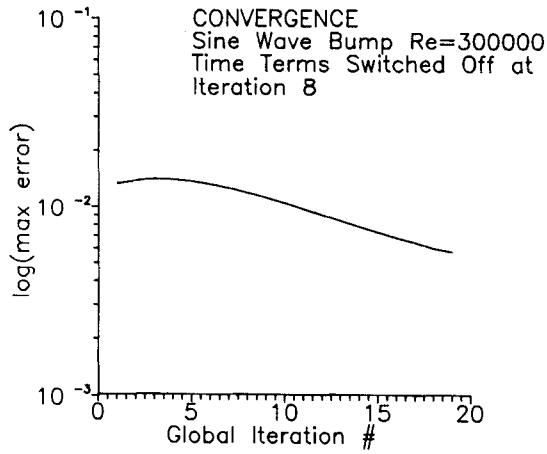

Figure 4. Convergence history: separated case

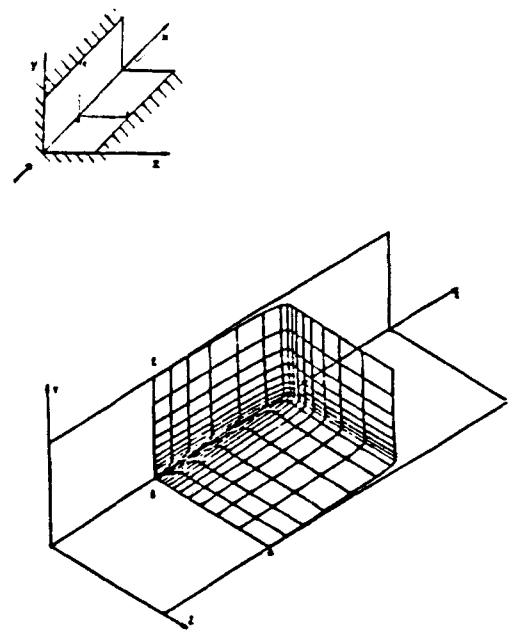

Figure 5. Streamwise velocity profile for an axial corner

the non-dimensional normal co-ordinate η at several ζ-locations, where

$$\eta = y\sqrt{Re/2x}, \qquad \zeta = z\sqrt{Re/2x}.$$

Streamwise velocity profiles for the finite plate are given in Figure 8, where comparison of the symmetry line profile to the Blasius solution[15] is shown.

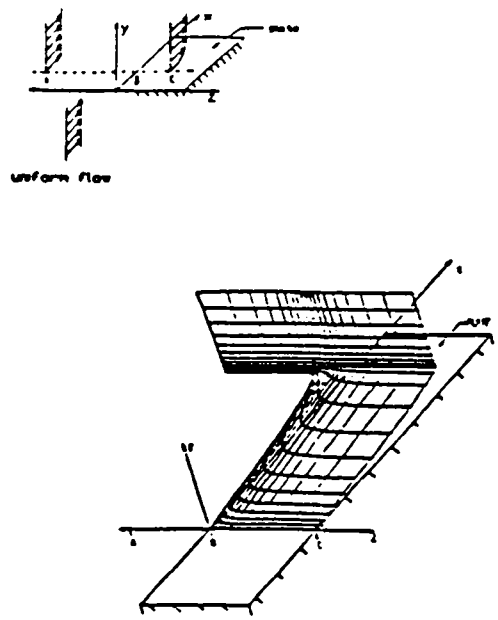

Figure 6. Streamwise velocity profile for a finite span plate

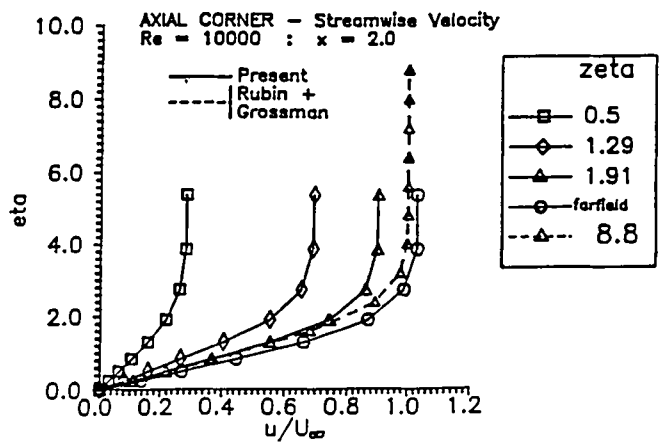

Figure 7. Corner flow velocity profiles

3.2. Separated flows

Following work by Smith,[16] Ramakrishnan and Rubin[5] and the present authors[17] on two-dimensional sine wave aerofoils, a three-dimensional configuration was chosen (Figure 9). A sine wave aerofoil in the streamwise direction with a trigonometric thickness variation in the spanwise direction was used. The body shape was given by

$$y_{\text{body}} = \begin{cases} 0, & x < 0, \\ \frac{1}{4}\text{TC}\{1 + \sin[2\pi(x - \frac{1}{2})]\}, & 0 < x < 1, \\ 0, & x > 1, \end{cases}$$

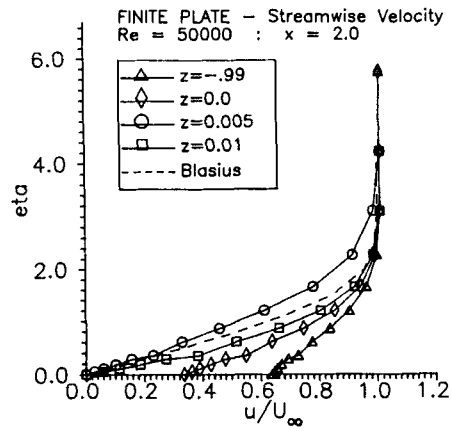

Figure 8. Finite span plate velocity profiles

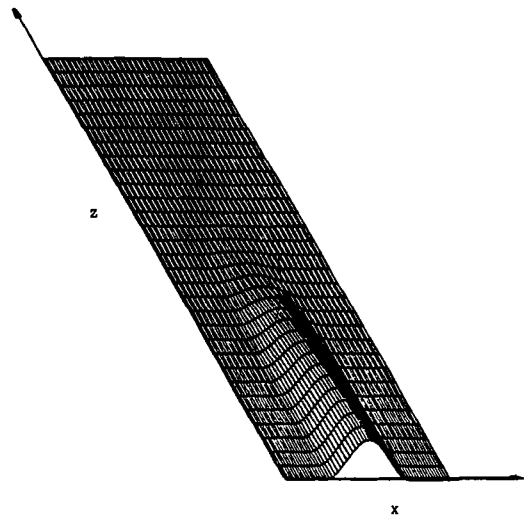

Figure 9. Three-dimensional bump configuration

where TC is the thickness to chord ratio of a double-sided aerofoil. Spanwise variation was given by varying the thickness ratio TC in the z-direction:

$$\mathrm{TC} = \begin{cases} (\mathrm{TC_r} - \mathrm{TC_t})\{1 + \sin[\pi(z/z_{\mathrm{ns}} + \frac{1}{2})]\} + \mathrm{TC_t}, & 0 < z < z_{\mathrm{ns}}, \\ \mathrm{TC_t}, & z > z_{\mathrm{ns}}, \end{cases}$$

where $\mathrm{TC_r}$ is the thickness ratio at the root ($z = 0$) and $\mathrm{TC_t}$ is the tip thickness ratio, which is constant from $z = z_{\mathrm{ns}}$ to the outer span. A non-orthogonal transformation in the cross-plane and a shearing transformation in the streamwise direction were implemented. These mapped the physical domain onto a rectangular computational domain.

The viscous flow field over this 'bump' configuration has a reversed flow bubble which decreases when moving from the symmetry line to the outer span. The bubble can be seen in

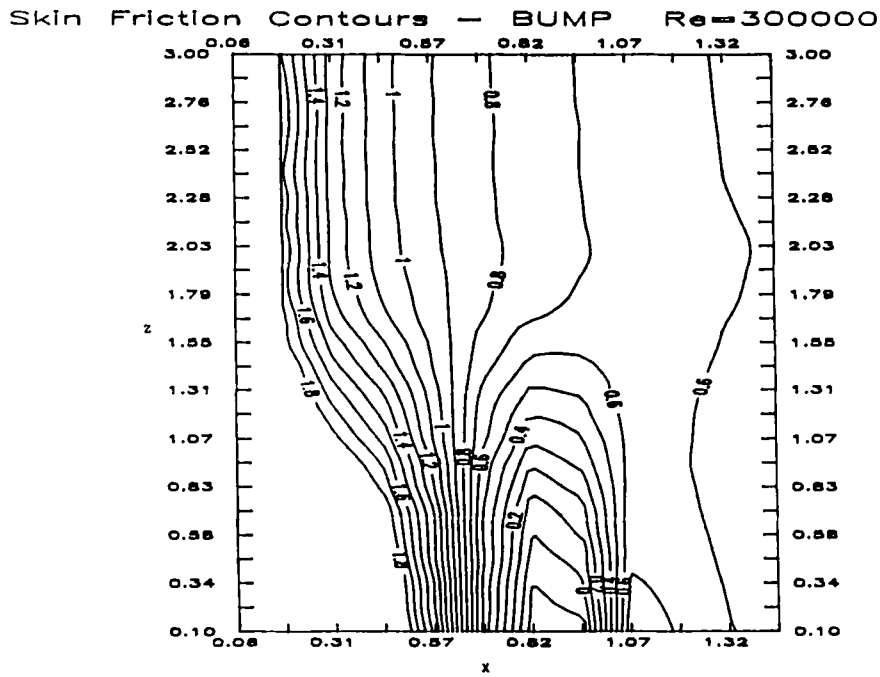

Figure 10. Skin friction contours for bump

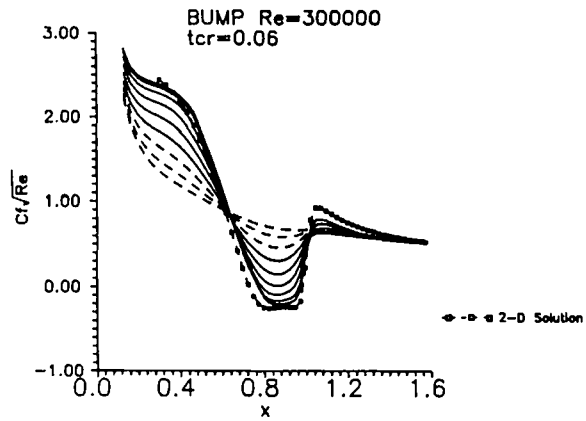

Figure 11. Skin friction for bump

surface skin fraction contour plots (Figure 10). Also shown are skin friction curves at different spanwise locations (Figure 11). These are compared to the skin friction on a two-dimensional sine wave aerofoil. The three-dimensional flow on the symmetry line of the bump exhibited a less severe reversed flow region than the two-dimensional configuration. This is due to the cross-flow present in the three-dimensional situation. Typical velocity profiles at a streamwise location where there is separated flow are also shown (Figure 12).

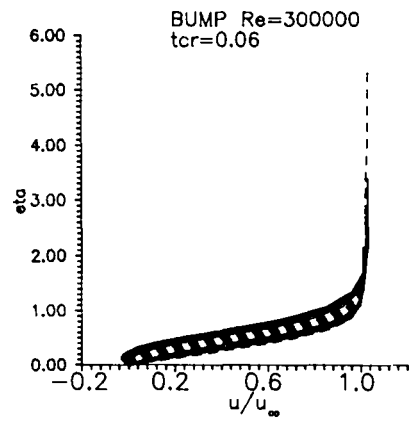

Figure 12. Velocity profiles for bump

4. COMPUTATION

Computer time is dominated by the matrix LU decomposition. The YSMP requires a large work vector for use during the matrix LU decomposition. This means that the number of unknowns in a given problem, and hence the grid size, is restricted by the capacity of the computer being used. The length of this vector was found to be about ten times the number of non-zero terms in the matrix A for the present scheme. The computations have been run on grids with 61 points in the streamwise direction. The largest corner flow was calculated on a 24×24 grid, while a 51×31 grid has been used for the other configurations. The corner flows were run on a personal computer with a Definicon DSI-68020 coprocessor board (20 MHz version) with four megabytes of internal memory. The number of unknowns was about 2300 (24×24 grid points with four unknowns at each point). Larger grids would still be solvable on the PC. For the larger cross-plane grids, a DEC Microvax 2 with 8 Mbytes of RAM was used. A CSPI 6420 array processor with 16 Mbytes of central memory is installed on this system. Without the array processor the computational speed of the PC is about 20% faster than the Microvax. A 21×21 system takes about 2.5 min for each cross-plane solution on the PC. The array processor runs about four times faster. Calculations for the bump configuration were performed on the Microvax with array processor. A cross-plane of 51×31 grid points (about 6000 unknowns) required about 5·5 min per marching step.

5. CONCLUSIONS

The current method has enabled calculation of three-dimensional separated and attached flows. Addition of time derivative terms and flux switching the differencing of convective terms in the streamwise and cross-flow momentum equations, where the flow is recirculating, makes the solution technique suitably robust. Using this method it is possible to obtain three-dimensional solutions with limited computer facilities.

ACKNOWLEDGEMENTS

The authors would like to thank Professor S. G. Rubin for many useful discussions, and also Erich Bender for his help in implementing the YSMP for these applications. This work was

supported by the AFOSR under contract number F49620-85-C-0027. Research was carried out while R. Cohen was at the University of Cincinnati under a Fulbright postgraduate award.

REFERENCES

1. S. G. Rubin, 'Incompressible Navier–Stokes and parabolized Navier–Stokes formulations', in W. G. Hubashi (ed.), *Computational Methods in Viscous Flows*, Pineridge Press, Swansea, 1984.
2. S. G. Rubin and A. Lin, 'Marching with the PNS equations', *Israel J. technol.*, **18**, 21–31 (1980).
3. S. G. Rubin and D. R. Reddy, 'Global solution procedure for incompressible laminar flow with strong pressure interaction and separation', *2nd Symp. on Numerical and Physical Methods for Aerodynamic Flows*, Long Beach, CA, 1983.
4. P. K. Khosla and H. T. Lai, 'Global PNS solutions for subsonic strong interaction flow over a cone–cylinder–boattail configuration', *Comput. Fluids*. **11**, 325 (1983).
5. S. V. Ramakrishnan and S. G. Rubin, 'Global pressure relaxation for steady, compressible, laminar, 2-dimensional flows with full pressure coupling and shock waves', *Report AFL-84-100*, University of Cincinnati, 1984.
6. S. Lubard and W. S. Helliwell, 'Calculation of the flow on a cone at high angle of attack', *AIAA J.*, **12**, 7 (1974).
7. H. C. Raven and M. Hoekstra, 'A parabolised Navier–Stokes solution method for ship stern calculations', *MARIN Report No. 50402-I-SR*, 1984; presented at *Second Int. Symp. on Ship Viscous Resistance*, Göteborg, March 1985.
8. M. Rosenfeld, M. Israeli and M. Wolfshtein, 'A numerical method for the solution of three dimensional, incompressible, viscous flows over slender bodies', preliminary version (1987).
9. H. L. Stone, 'Iterative solution of implicit approximations of multi-dimensional partial differential equations', *SIAM J. Numer. Anal.*, **5**, 530–558 (1960).
10. P. K. Khosla and S. G. Rubin, 'Consistent strongly implicit procedures', presented at *10th Int. Conf. on Numerical Methods in Fluid Dynamics*, Beijing, June 1986.
11. S. C. Eisinstadt, M. C. Gursky, M. H. Schultz and A. H. Sherman, 'Yale sparse matrix package II. The nonsymmetric codes', *Yale University Department of Computer Science Research Report # 114*, 1977.
12. E. E. Bender and P. K. Khosla, 'Solution of the two-dimensional Navier–Stokes equations using sparse matrix solvers', *AIAA Paper No. 86-0603*, 1986; presented at *25th Aerospace Sciences Meeting*, Reno, Nevada, January 1987.
13. S. P. Vanka and G. K. Leaf, 'Fully coupled solution of pressure-linked fluid flow equations', *Report ANL-83-73*, Argonne National Laboratory, Argonne, IL, 1983.
14. S. G. Rubin and B. Grossman, 'Viscous flow along a corner: numerical solution of the corner layer equations', *Q. Appl. Math.*, **29**, 169–186 (1971).
15. H. Schlichting, *Boundary Layer Theory*, 7th Edn, McGraw-Hill, 1979, pp. 137–139.
16. F. T. Smith, 'Laminar flow of an incompressible fluid past a bluff body: the separation, reattachment, eddy-properties and drag', *J. Fluid Mech.*, **92**, (1979).
17. R. Cohen and P. K. Khosla, 'Solution to the reduced Navier Stokes equations in three dimensions, using a global relaxation procedure in C. A. J. Fletcher (ed.), *Proc. CTAC-87/ISCFD*, Sydney, August 1987, to be published.
18. D. A. Anderson, J. C. Tannehill and R. H. Pletcher, *Computational Fluid Mechanics and Heat Transfer*, McGraw-Hill 1984.